Mathematisches
Forschungsinstitut
Oberwolfach

Oberwolfach Preprints

HANSJÖRG GEIGES AND SINEM ONARAN

Exceptional Legendrian Torus Knots

Oberwolfach Preprints (OWP)

Starting in 2007, the MFO publishes a preprint series which mainly contains research results related to a longer stay in Oberwolfach. In particular, this concerns the Research in Pairs-Programme (RiP) and the Oberwolfach-Leibniz-Fellows (OWLF), but this can also include an Oberwolfach Lecture, for example.

A preprint can have a size from 1 - 200 pages, and the MFO will publish it on its website as well as by hard copy. Every RiP group or Oberwolfach-Leibniz-Fellow may receive on request 30 free hard copies (DIN A4, black and white copy) by surface mail.

Of course, the full copy right is left to the authors. The MFO only needs the right to publish it on its website *www.mfo.de* as a documentation of the research work done at the MFO, which you are accepting by sending us your file.

In case of interest, please send a **pdf file** of your preprint by email to *rip@mfo.de* or *owlf@mfo.de*, respectively. The file should be sent to the MFO within 12 months after your stay as RiP or OWLF at the MFO.

There are no requirements for the format of the preprint, except that the introduction should contain a short appreciation and that the paper size (respectively format) should be DIN A4, "letter" or "article".

On the front page of the hard copies, which contains the logo of the MFO, title and authors, we shall add a running number (20XX - XX).

We cordially invite the researchers within the RiP or OWLF programme to make use of this offer and would like to thank you in advance for your cooperation.

EXCEPTIONAL LEGENDRIAN TORUS KNOTS

HANSJÖRG GEIGES AND SINEM ONARAN

ABSTRACT. We present classification results for exceptional Legendrian realisations of torus knots. These are the first results of that kind for non-trivial topological knot types. Enumeration results of Ding–Li–Zhang concerning tight contact structures on certain Seifert fibred manifolds with boundary allow us to place upper bounds on the number of tight contact structures on the complements of torus knots; the classification of exceptional realisations of these torus knots is then achieved by exhibiting sufficiently many realisations in terms of contact surgery diagrams. We also discuss a couple of general theorems about the existence of exceptional Legendrian knots.

1. INTRODUCTION

The classification of Legendrian knots is one of the basic questions in 3-dimensional contact topology. The first classification result — for Legendrian realisations of the topological unknot in the 3-sphere S^3 with its standard tight contact structure ξ_{st} — is due to Eliashberg and Fraser [13]; see also [14]. Legendrian realisations of torus knots and the figure eight knot in (S^3, ξ_{st}) were classified by Etnyre and Honda [16]. In those topological knot types one can determine the range of the classical invariants tb (Thurston–Bennequin invariant) and rot (rotation number), and it is shown that these invariants suffice to distinguish the knots up to Legendrian isotopy.

In general, further invariants are required for a complete classification. The first example of that kind was discovered by Chekanov [3] and Eliashberg: there are two Legendrian realisations of the 5_2 knot with the same classical invariants that can be distinguished by a differential graded algebra associated with the Legendrian knot.

The Legendrian classification question can be extended in various directions: Legendrian links [6], knots or links in other tight contact 3-manifolds [1, 4, 8, 24, 32], or knots in overtwisted contact structures [14, 15, 21]. Here we have only cited a few examples where again the classical invariants suffice to distinguish all Legendrian realisations.

Knots of the latter kind are the object of interest in this paper. They fall into two classes.

Definition 1.1. A Legendrian knot L in an overtwisted contact 3-manifold (M, ξ) is called *exceptional* (or *non-loose*) if its complement $(M \setminus L, \xi|_{M \setminus L})$ is tight; L is called *loose* if the contact structure is still overtwisted when restricted to the knot complement.

As shown by Etnyre [15, Theorem 1.4], loose Legendrian knots in null-homologous knot types in any contact 3-manifold are classified by the classical invariants (and the range of the invariants is only restricted by $\mathtt{tb} + \mathtt{rot}$ being odd). See also [12, Theorem 0.1] and [7, Theorem 6].

Remark 1.2. Here by 'classification' we always mean the classification of *oriented* Legendrian knots up to *coarse equivalence*, i.e. up to contactomorphism of the ambient manifold. Since the contactomorphism groups of contact manifolds other than (S^3, ξ_{st}) are not, in general, connected, the classification up to Legendrian isotopy is more subtle.

The classification of exceptional Legendrian knots is more involved than that of loose ones. Exceptional topological unknots were classified by Eliashberg and Fraser [14]; see [21, Theorem 5.1] for an alternative argument. Recall that, up to isotopy, there is an integer family of overtwisted contact structures on S^3, which are distinguished by the Hopf invariant $h \in \mathbb{Z}$ of the underlying tangent 2-plane field. We work instead with the d_3-invariant (see [9] for its general definition); for S^3 the two invariants are related by $d_3 = -h - 1/2$. We write ξ_d for the overtwisted contact structure on S^3 characterised by $d_3(\xi_d) = d \in \mathbb{Z} + 1/2$. The standard contact structure on S^3 has $d_3(\xi_{\mathrm{st}}) = -1/2$; thus, whenever we have a contact structure on S^3 (e.g. a structure obtained by one of the surgery diagrams used in this paper) with $d_3 \neq -1/2$, we know right away that the contact structure is overtwisted.

Theorem 1.3 (Eliashberg–Fraser)**.** *Let $L \subset (S^3, \xi)$ be an exceptional unknot in an overtwisted contact structure ξ on the 3-sphere. Then $\xi = \xi_{1/2}$, and the classical invariants can take the values*

$$\big(\mathtt{tb}(L), \mathtt{rot}(L)\big) \in \big\{(n, \pm(n-1))\colon n \in \mathbb{N}\big\}.$$

These invariants determine L up to coarse equivalence.

In [21] we classified exceptional rational unknots in lens spaces. In the present paper we achieve the first classification of exceptional realisations of non-trivial topological knot types.

One issue that did not arise in [14] or [21] was that of positive Giroux torsion (as defined in [26]), because there the knot complement was a solid torus, which would become overtwisted by introducing Giroux torsion along the boundary. For non-trivial topological knot types, exceptional Legendrian realisations may well have positive Giroux torsion in the complement.

As shown by Etnyre [15], see also the discussion in [33], one can produce infinitely many exceptional Legendrian knots — with the same classical invariants — that are not coarsely equivalent, by introducing Giroux torsion along an incompressible torus in the knot complement, which does not change the ambient contact structure.

When one wants to classify exceptional Legendrian realisations in a given topological knot type, it is therefore reasonable to impose the stronger condition that the knot complement is not only tight, but that it has zero Giroux torsion. Recall that overtwisted contact structures have infinite Giroux torsion. We adopt the following terminology from [33].

Definition 1.4. A Legendrian knot L in an overtwisted contact 3-manifold (M, ξ) is called *strongly exceptional* if its complement $(M \setminus L, \xi|_{M \setminus L})$ has zero Giroux torsion.

Even in the strongly exceptional case, the classical invariants may not distinguish all Legendrian realisations, as shown in [33].

Our aim in this paper will be to classify strongly exceptional realisations of certain torus knots. We begin in Section 2 with the observation that, as a consequence

of the Legendrian surgery presentation theorem [5, 9], any closed, overtwisted contact 3-manifold contains an exceptional Legendrian knot. (This also follows from the work of Etnyre and Vela-Vick [17].) In Section 3 we give a sufficient criterion for a topological knot type to admit an exceptional realisation.

The strategy for classifying exceptional torus knots is similar to the one we employed in [21] for the classification of exceptional rational unknots. The complement of a torus knot is a bounded 3-manifold that admits a Seifert fibration over the disc with two multiple fibres. For certain boundary conditions, the tight contact structures (of zero Giroux torsion) on such manifolds have been classified by Ding–Li–Zhang [10]. Their results give us an upper bound on the number of Legendrian realisations whose complement has zero Giroux torsion, in other words, strongly exceptional realisations or realisations in (S^3, ξ_{st}). Realisations of the latter kind have been classified, as mentioned before, by Etnyre–Honda [16]. It then remains to exhibit sufficiently many strongly exceptional realisations in terms of surgery diagrams. The new ingredient for establishing that the examples are indeed strongly exceptional is the LOSS invariant $\hat{\mathfrak{L}}$ from [28] and a vanishing theorem for $\hat{\mathfrak{L}}$ due to Stipsicz and Vértesi [33].

In Section 4 we describe the Seifert fibration of torus knot complements and summarise the relevant results from [10]. In Section 5 we then apply this to the left-handed trefoil knot; here the results of [10] allow the most comprehensive classification.

Theorem 1.5. *The number of strongly exceptional Legendrian realisations L of the left-handed trefoil knot in S^3 is as follows:*

(a) *For $\mathtt{tb}(L) = -5$ and $\mathtt{tb}(L) < -6$, there are precisely two such realisations; they live in $(S^3, \xi_{3/2})$.*
(b) *For $\mathtt{tb}(L) = 1$, there is at least one realisation.*
(c) *For each other value of $\mathtt{tb}(L) \in \mathbb{Z}$, there are at least two realisations.*

All the known exceptional realisations in cases (b) and (c) likewise live in the contact structure $\xi_{3/2}$ on S^3. Conjecturally, the examples we shall describe constitute a complete list of strongly exceptional realisations of the left-handed trefoil knot.

In Section 6 we discuss the classification of strongly exceptional right-handed trefoils. Finally, in Section 7 we give some classification results for two general classes of torus knots. Some of the detailed calculations of the classical invariants and the d_3-invariant are relegated to Section 8.

2. Existence of exceptional knots

The first example of an exceptional Legendrian knot was found by Dymara [12]. The intricacy of her construction could lead one to expect such knots to be scarce. The following theorem, however, shows that every overtwisted contact manifold contains an exceptional knot.

Theorem 2.1. *Any closed overtwisted contact 3-manifold contains an exceptional Legendrian knot.*

Proof. According to the surgery presentation theorem of [5], any closed contact 3-manifold (M, ξ) can be obtained by contact (± 1)-surgery on a suitable Legendrian link $\mathbb{L}$ in (S^3, ξ_{st}). As observed in [9, Corollary 1.4], one may choose the Legendrian

link $\mathbb{L}$ such that a contact $(+1)$-surgery on a single component L_0 of $\mathbb{L}$ and contact (-1)-surgeries on all other components produces the desired manifold (M, ξ).

The Legendrian push-off L of L_0 in (S^3, ξ_{st}) may be regarded as a Legendrian knot in the surgered manifold (M, ξ). By the cancellation lemma of [5], cf. [19, Proposition 6.4.5], contact (-1)-surgery on L cancels the contact $(+1)$-surgery on L_0. In other words, contact (-1)-surgery on $L \subset (M, \xi)$ produces the same contact manifold as contact (-1)-surgeries on $(\mathbb{L} \setminus L_0) \subset (S^3, \xi_{\mathrm{st}})$. Contact (-1)-surgery is symplectic handlebody surgery [19, Section 6.2], thus, the latter manifold is symplectically fillable and hence tight. In particular, the complement of L in (M, ξ) must have been tight. $\qquad\square$

Remark 2.2. The proof of [9, Corollary 1.4] implicitly relies on the theory of open books adapted to contact structures. For a proof entirely in the surgical realm see [23, Theorem 3.4].

The explicit realisations of exceptional knots in the present paper will be based on the idea in the proof of the theorem above. The following proposition says that exceptional knots realised in that fashion will always be *strongly* exceptional.

Proposition 2.3. *Let (M, ξ) be an overtwisted contact 3-manifold represented by a contact (± 1)-surgery diagram containing a single $(+1)$-surgery. Then the Legendrian knot L in (M, ξ) represented by the push-off of the $(+1)$-surgery curve is strongly exceptional.*

Proof. In the foregoing proof we have seen that contact (-1)-surgery along L produces a strongly symplectically fillable contact 3-manifold. As shown by Gay [18, Corollary 3], positive Giroux torsion obstructs strong fillability. Thus, contact (-1)-surgery along L produces a manifold with zero Giroux torsion. In particular, the complement of L in (M, ξ) must have been of zero Giroux torsion. $\qquad\square$

Remark 2.4. For an alternative proof of the existence of a strongly exceptional Legendrian knot in any given closed overtwisted contact 3-manifold (M, ξ) one may appeal to [17, Theorem 1.2], which says that the binding B of any open book decomposition of M supporting ξ has zero Giroux torsion in its complement, i.e. B is a strongly exceptional transverse knot. By [15, Proposition 1.2], any Legendrian approximation of B is then likewise strongly exceptional. (That proposition is formulated for exceptional rather than strongly exceptional knots, but the proof also works in the strongly exceptional case.)

Even though all closed overtwisted contact 3-manifolds contain exceptional Legendrian knots, the two theorems in the introduction indicate that on a given differential manifold (here: the 3-sphere), exceptional realisations of a given knot type may exist in only one or very few overtwisted contact structures. The examples below will confirm this observation. This suggests that the 'most simple' exceptional knot in an overtwisted contact structure is a measure for its complexity.

3. Exceptional knots in $(S^3, \xi_{1/2})$

By Theorem 1.3, the contact structure $\xi_{1/2}$ is distinguished as the only overtwisted contact structure on S^3 containing exceptional realisations of the topological unknot. The following proposition gives a sufficient criterion for a topological knot type to admit an exceptional Legendrian realisation in $(S^3, \xi_{1/2})$.

Proposition 3.1. *Let L be a Legendrian knot in (S^3, ξ_{st}). If contact $(+1)$-surgery on L produces a tight contact 3-manifold, then the topological knot type of L admits an exceptional realisation in $(S^3, \xi_{1/2})$.*

Proof. Given $L \subset (S^3, \xi_{st})$, perform two contact $(+1)$-surgeries along a standard Legendrian meridian and its push-off as shown in Figure 1. The Kirby moves in Figure 2 show that the surgered manifold is again the 3-sphere, and the topological knot type of L is not affected by the surgeries. From the formula in [9, Corollary 3.6] (see equation (5) below) it follows that the d_3-invariant of the surgered contact structure equals $1/2$.
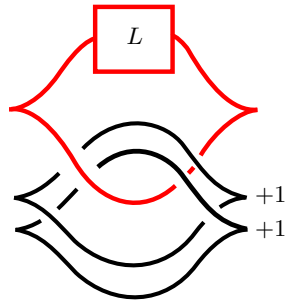

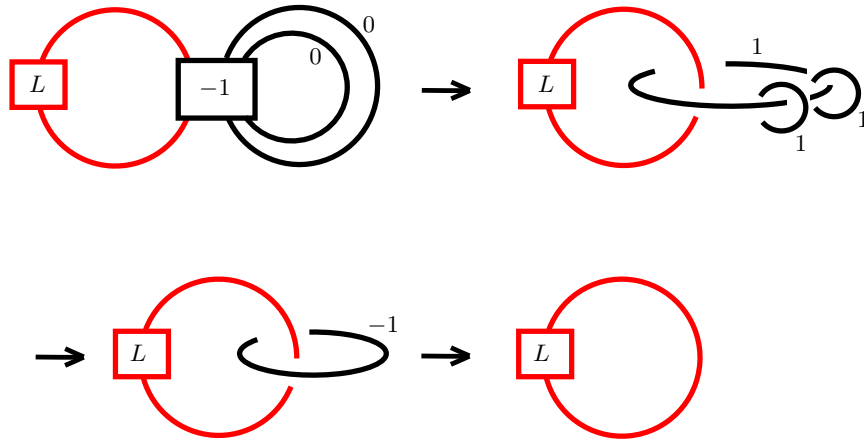FIGURE 1. A Legendrian knot L in $(S^3, \xi_{1/2})$.

FIGURE 2. The topological type of (S^3, L) is unchanged by the surgery.

In order to see that $L \subset (S^3, \xi_{1/2})$ is exceptional, we perform contact (-1)-surgery on L (in addition to the two $(+1)$-surgeries). By [7, Proposition 2], in the contact manifold obtained (from any initial contact manifold) by a contact (-1)-surgery along a Legendrian knot K, the standard Legendrian meridian of K is Legendrian isotopic to the Legendrian push-off of K. Thus, surgery along the three knots as described is equivalent to a (-1)-surgery along L and $(+1)$-surgeries along two push-offs of L. By the cancellation lemma, this amounts to a single $(+1)$-surgery on L in (S^3, ξ_{st}).

In conclusion, if contact $(+1)$-surgery on $L \subset (S^3, \xi_{\mathrm{st}})$ produces a tight contact 3-manifold, then so does (-1)-surgery on $L \subset (S^3, \xi_{1/2})$, which proves this latter realisation of L to be exceptional. $\qquad\square$

Example 3.2. The basic example for this proposition is provided by the topological unknot. Contact $(+1)$-surgery along its Legendrian realisation in (S^3, ξ_{st}) with $\mathtt{tb} = -1$ produces the tight contact structure on $S^1 \times S^2$.

Further examples are supplied by a theorem of Lisca and Stipsicz. Let K be a knot in S^3 with positive slice genus $g_s > 0$ and maximal Thurston–Bennequin invariant $\overline{\mathtt{tb}}$ (of Legendrian realisations in (S^3, ξ_{st})) equal to $2g_s - 1$. Then by [29, Theorem 1.1] and its proof, contact r-surgery with $r \neq 0$ along a Legendrian realisation L of K with $\mathtt{tb}(L) = \overline{\mathtt{tb}}$ yields a tight contact structure. This result applies, for instance, to all positive (p, q)-torus knots, $p, q \geq 2$, whose slice genus equals $g_s = (p-1)(q-1)/2$, and whose maximal Thurston–Bennequin invariant is $\overline{\mathtt{tb}} = pq - p - q = 2g_s - 1$ by [16, Theorem 4.1].

In a different context, these examples have previously been observed in [2, Example 4.1.13].

4. Exceptional torus knots

In this section we provide some background for the study of exceptional realisations of torus knots.

4.1. **Seifert fibrations of torus knot complements.** For given coprime integers p, q, consider the S^1-action on $S^3 \subset \mathbb{C}^2$ given by

$$\theta(z_1, z_2) = (\mathrm{e}^{\mathrm{i}p\theta} z_1, \mathrm{e}^{\mathrm{i}q\theta} z_2), \quad \theta \in S^1 = \mathbb{R}/2\pi\mathbb{Z}.$$

This defines a Seifert fibration with two singular fibres of multiplicity $|p|$ and $|q|$ through the points $(1, 0)$ and $(0, 1)$, respectively. All regular fibres are copies of the (p, q)-torus knot.

Choose integers p', q' such that $pq' + p'q = 1$. Then, with the conventions of [20, Section 2.2], the Seifert invariants are given by

$$\big(g = 0; (1, 0), (p, p'), (q, q')\big),$$

where we include a Seifert pair $(1, 0)$, corresponding to a non-singular fibre, to represent a copy K of the (p, q)-torus knot. In particular, the complement of K is Seifert fibred. Notice that by [30], the property of having a Seifert fibred complement characterises torus knots.

Let νK be a closed tubular neighbourhood of K made up of Seifert fibres. The Seifert fibration on $S^3 \setminus \mathrm{Int}(\nu K)$ has base D^2 and two singular fibres. In terms of the invariants used in [10, Section 2], this Seifert fibration is $M(D^2; -p'/p, -q'/q)$; this follows by comparing the conventions there with those of [20, Section 2.2].

Write μ for the meridian on the boundary $\partial(\nu K)$ of the tubular neighbourhood; as a longitude λ we choose a parallel Seifert fibre, so that the linking number between K and λ is $\mathtt{lk}(K, \lambda) = pq$. On the complement $M(D^2; -p'/p, -q'/q)$, the meridian μ is identified with $-\partial D^2 \times \{1\}$; the longitude λ corresponds to an S^1-fibre $\{*\} \times S^1$ for some point $* \in \partial D^2$.

In [10], the authors determine the number of tight contact structures on the Seifert fibred manifold $M(D^2; -p'/p, -q'/q)$ with minimal convex boundary of slope s and zero Giroux torsion along the boundary, for a certain range of permissible slopes. 'Minimality' of the boundary means that there are two dividing

curves. The slope of the dividing curves is measured with respect to the basis (μ, λ) (under the above identifications).

Now let $L \subset (S^3, \xi)$ be a Legendrian realisation of the (p, q)-torus knot K in some contact structure ξ on the 3-sphere. The boundary of a standard tubular neighbourhood of L is minimal convex. Write λ_s, λ_c for the curves on $\partial(\nu L)$ representing the surface framing and the contact framing, respectively. From $\mathtt{lk}(K, \lambda) = pq$ we have

$$\lambda_s = \lambda - pq\mu.$$

Hence

$$\lambda_c = \lambda_s + \mathtt{tb}(L)\mu = \lambda + (\mathtt{tb}(L) - pq)\mu.$$

So the slope s is given by

$$s = \frac{1}{\mathtt{tb}(L) - pq}.$$

4.2. Two families of torus knots.

We now consider two families of torus knots, where, as we shall see, the classification results of Ding–Li–Zhang [10] about tight contact structures on certain Seifert fibred manifolds with torus boundary apply, and exceptional realisations can be described in surgery diagrams.

4.2.1. *Positive torus knots.* We first look at positive (p, q)-torus knots, where p is a natural number greater than or equal to 2, and $q = np + 1$ for some $n \in \mathbb{N}$. This means that $p \cdot (-n) + 1 \cdot q = 1$, so in the notation of Section 4.1 we have $p' = 1$ and $q' = -n$. Hence, we would like to determine the number of tight contact structures on

$$M\left(D^2; -\frac{1}{p}, \frac{n}{np+1}\right) \quad \text{of boundary slope} \quad s = \frac{1}{\mathtt{tb}(L) - pq}.$$

(The condition 'zero Giroux torsion along the boundary' will be understood from now on.) By [10, Proposition 2.2], this is the same as the number of tight structures on

$$(1) \qquad M\left(D^2; \frac{p-1}{p}, \frac{n}{np+1}\right) \quad \text{of boundary slope} \quad s = \frac{1}{\mathtt{tb}(L) - pq} + 1.$$

The Seifert invariant $r_1 := (p-1)/p$ lies in the interval $[1/2, 1)$, the invariant $r_2 := n/(np+1)$, in $(0, 1/2)$. It follows that the only case of the classification in [10] that applies is their case (1), where the concrete values of the Seifert invariants r_1, r_2 (in the range $(0, 1) \cap \mathbb{Q}$) are irrelevant, but the slope s has to satisfy

$$(\text{DLZ1}) \qquad\qquad s \in (-\infty, 0) \cup [2, \infty).$$

The slope in equation (1) lies in $[0, 2] \cup \{\infty\}$, so the only case where the classification applies is

$$\mathtt{tb}(L) = pq + 1 = np^2 + p + 1,$$

when $s = 2$.

4.2.2. *Negative torus knots.* We consider negative (p, q)-torus knots with $p \geq 2$ and $q = -(np - 1)$ for some $n \geq 2$. We have $p \cdot n + 1 \cdot q = 1$, so that $p' = 1$ and $q' = n$. This requires us to find the tight contact structures on

$$M\left(D^2; -\frac{1}{p}, \frac{n}{np - 1}\right) \quad \text{of boundary slope} \quad s = \frac{1}{\mathtt{tb}(L) - pq},$$

or on

$$(2) \qquad M\left(D^2; \frac{p - 1}{p}, \frac{n}{np - 1}\right) \quad \text{of boundary slope} \quad s = \frac{1}{\mathtt{tb}(L) - pq} + 1.$$

The value

$$\mathtt{tb}(L) = pq + 1 = -np^2 + p + 1$$

gives us $s = 2$, so we are again in the case (DLZ1), with no restriction on the Seifert invariants.

The Seifert invariant $r_1 := (p - 1)/p$ lies in the interval $[1/2, 1)$, and for $p \geq 3$ the Seifert invariant $r_2 := n/(np - 1)$, in the interval $(0, 1/2)$. This means that no other case of the classification in [10] applies.

For $p = 2$ we have $1/2 < r_2 < 1$ for all n, so we are in case (2) of [10]:

$$(\text{DLZ2}) \qquad\qquad\qquad r_1, r_2 \in [1/2, 1) \quad \text{and} \quad s \in [0, 1).$$

With equation (2) the slope condition $s \in [0, 1)$ translates into $\mathtt{tb}(L) < -p(np - 1)$.

5. Exceptional left-handed trefoils

The discussion in the previous section suggests as potentially worthwhile the study of exceptional left-handed trefoils, i.e. $(2, -3)$-torus knots, subject to the condition $\mathtt{tb}(L) = -5$ or $\mathtt{tb}(L) < -6$. The aim of this section is to prove Theorem 1.5, which shows that here a complete classification is indeed possible.

As we shall see in the course of the proof, explicit realisations of the two exceptional left-handed trefoils with $\mathtt{tb} < -6$ are given as follows. The left-handed trefoil L in Figure 3, taken from [22], is strongly exceptional with $\mathtt{tb}(L) = -6$. With the clockwise orientation it has $\mathtt{rot}(L) = -7$. Its negative stabilisations are strongly exceptional, with $(\mathtt{tb}, \mathtt{rot}) = (-6 - k, -7 - k)$. The second strongly exceptional realisation is given by reversing the orientation, so that $(\mathtt{tb}, \mathtt{rot}) = (-6 - k, 7 + k)$.

5.1. **Number of tight structures on the knot complement.** In the notation of Section 4.2.2 we take $p = 2$ and $n = 2$, so that $q = -(np - 1) = -3$. The knot complement of a Legendrian $(2, -3)$-torus knot L is the Seifert manifold $M(D^2; 1/2, 2/3)$, with boundary slope $s = 1 + 1/(\mathtt{tb}(L) + 6)$.

5.1.1. *The case* $\mathtt{tb}(L) = -5$. Here we have slope $s = 2$. Following the algorithm of [10, p. 65], we write the number $s - [s]$ as b/a with integers $a > b \geq 0$, so we may take $a = 1, b = 0$, and then set

$$a_1 = \frac{1}{1 - b/a} + 1 = 2, \quad a_2 = 1.$$

Moreover, by [10, p. 68], we have to write down negative continued fraction expansions of the $-1/r_i$, $i = 1, 2$. For $r_1 = 1/2$ this gives us $a_0^1 = -2$. For $r_2 = 2/3$ we have
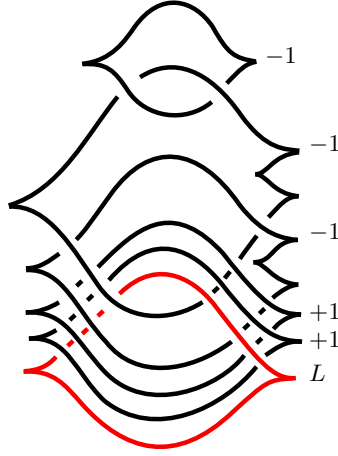
$$-\frac{3}{2} = -2 - \frac{1}{-2},$$

FIGURE 3. An exceptional left-handed trefoil L with $\mathtt{tb} = -6$.

that is, $a_0^2 = a_1^2 = -2$. By formula $(***)$ on p. 75 of [10], there are exactly

$$[s] \prod_{i,j} |a_j^i + 1|(a_1 - 1)a_2 = 2$$

tight contact structures.

5.1.2. *The case* $\mathtt{tb}(L) < -6$. For $\mathtt{tb}(L) = -6 - k$, $k \in \mathbb{N}$, the corresponding slope $s = s_k$ is given by

$$s = \frac{1}{-k} + 1 = \frac{k-1}{k}.$$

Now, according to [10, Theorem 1.1], the number of tight contact structures, up to isotopy fixing the boundary, on $M(D^2; 1/2, 2/3)$ equals the number of tight contact structures, up to isotopy, on the small Seifert manifold

$$M\left(-1 - [s]; \frac{1}{2}, \frac{2}{3}, r_3\right),$$

where the Seifert invariant r_3 is determined as follows.

Choose integers $a > b \geq 0$ such that

$$\frac{b}{a} = s - [s] = \frac{k-1}{k}.$$

This means $a = k$, $b = k - 1$. Then

$$\frac{1}{1 - b/a} = k$$

is an integer, so the recipe of [10, p. 65] again tells us to set

$$a_1 = \frac{1}{1 - b/a} + 1 = k + 1, \quad a_2 = 1,$$

and to define

$$r_3 = \cfrac{1}{a_1 - \cfrac{1}{a_2 + 1}} = \frac{2}{2k + 1}.$$

The number of tight contact structures on the Seifert manifold

$$M\left(-1; \frac{1}{2}, \frac{2}{3}, \frac{2}{2k+1}\right)$$

has been determined in [25, Theorem 1.1]. The formula given there is elementary but quite involved, so we leave it to the reader to check our calculation, which gives $k + 4$ tight contact structures. Beware that the calculations in [25] presume that the Seifert invariants are ordered in size, so one needs to work with

$$(r_1, r_2, r_3) = (2/3, 1/2, 2/2k+1)$$

for $k \geq 2$, and with

$$(r_1, r_2, r_3) = (2/3, 2/3, 1/2)$$

for $k = 1$.

5.2. Realisations in the standard contact structure.

The Legendrian realisations of the left-handed trefoil knot in (S^3, ξ_{st}) have been classified by Etnyre and Honda [16]. Here is a paraphrase of their Theorems 4.3 and 4.4.

Theorem 5.1 (Etnyre–Honda). *The Legendrian realisations L of the left-handed trefoil knot in (S^3, ξ_{st}) are determined, up to Legendrian isotopy, by their classical invariants in the range*

$$\mathtt{tb}(L) = -6 - k, \quad k \in \mathbb{N}_0,$$

and, correspondingly,

$$\mathtt{rot}(L) \in \{-(k+1), -(k-1), \ldots, k-1, k+1\}.$$

This means that for $\mathtt{tb}(L) = -6 - k$ there are $k + 2$ distinct realisations.

5.3. The LOSS invariant.

In [28], Lisca *et al.* introduced an invariant $\hat{\mathfrak{L}}$ for oriented, homologically trivial Legendrian knots L in an arbitrary closed contact 3-manifold (M, ξ), taking values in certain Heegaard Floer homology groups, with the following properties:

  (i) If $\hat{\mathfrak{L}}(L) \neq 0$ and ξ is overtwisted, then L is exceptional [28, Theorem 1.4].
  (ii) The negative stabilisation $S_- L$ of L has the same LOSS invariant:
      $\hat{\mathfrak{L}}(S_- L) = \hat{\mathfrak{L}}(L)$ [28, Theorem 1.6].

Moreover, in [28, Theorem 6.8] they established that the Legendrian knot L in Figure 3 with the clockwise orientation has $\hat{\mathfrak{L}}(L) \neq 0$. The rotation number of L is found with the formula in [28, Lemma 6.6] to be $\mathtt{rot}(L) = -7$. (See equation (4) below for this formula.)

With the properties (i) and (ii) of $\hat{\mathfrak{L}}$ we conclude that the negative stabilisations of L give us exceptional Legendrian left-handed trefoils with $(\mathtt{tb}, \mathtt{rot})$ taking the values $(-6 - k, -7 - k)$, $k \in \mathbb{N}$. Reversing the orientation of these knots gives exceptional trefoils with $(\mathtt{tb}, \mathtt{rot}) = (-6 - k, 7 + k)$.

Remark 5.2. The vanishing theorem [33, Corollary 1.2] guarantees that a (homologically trivial) Legendrian knot L with $\hat{\mathfrak{L}}(L) \neq 0$ is in fact *strongly* exceptional.

5.4. **Proof of Theorem 1.5.** For $\mathtt{tb}(L) = -6-k$, $k \in \mathbb{N}$, we found in Section 5.1.2 that there are at most $k+4$ Legendrian realisations with zero Giroux torsion in the complement. Theorem 5.1 gives us $k+2$ realisations in ξ_{st}, so there can be at most two strongly exceptional realisations. These are the two described in Section 5.3 and detected by the LOSS invariant.

The examples in Section 5.3 include the case $\mathtt{tb} = -6$ (as shown in Figure 3).

Remark 5.3. From our discussion we can conclude that the knot $-L$, i.e. the knot in Figure 3 with the counter-clockwise orientation has $\hat{\mathfrak{L}}(-L) = 0$. For otherwise the negative stabilisations of $-L$ would likewise be strongly exceptional. This would give more strongly exceptional realisations than allowed by the arithmetic in Section 5.1. For instance, for $\mathtt{tb} = -7$ there can be at most five Legendrian realisations of the left-handed trefoil with complement having zero Giroux torsion. The three realisations in ξ_{st} have $\mathtt{rot} \in \{0, \pm 2\}$. The exceptional knots $\pm S_- L$ in $\xi_{3/2}$ have $\mathtt{rot} = \pm 8$. The knot $S_-(-L) = -S_+ L$ has $\mathtt{rot} = 6$, so it must be distinct from the other five, and hence loose.

For $\mathtt{tb}(L) = -5$ there can be at most two strongly exceptional realisations of the left-handed trefoil by the calculation in Section 5.1.1. Explicit realisations, as we shall explain, are given in Figure 4 (with the two choices of orientation for L).
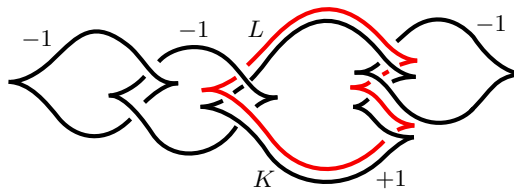

FIGURE 4. The two exceptional left-handed trefoils L with $\mathtt{tb} = -5$.

For the other values of $\mathtt{tb}(L)$, examples of strongly exceptional realisations are given in Figure 5. Here m denotes the number of Legendrian unknots with $\mathtt{tb} = -1$ in the vertical chain; notice that for $m = 0$ this figure specialises to Figure 4.

Lemma 5.4. *The knot L in the surgery diagram of Figure 5 — including the case $m = 0$, shown separately in Figure 4 — is a left-handed trefoil in the 3-sphere.*

Proof. The knot L has linking -2 with the surgery curve K at the bottom of the picture, whose topological surgery framing is -1. By blowing up twice, so that we place two $(+1)$-framed meridians around K, we can turn L into a parallel curve of K (with zero linking), and the surgery framing of K has changed to $+1$. A handle slide of L over K will then turn L into a meridian of K, unlinked from the next surgery curve and the two $(+1)$-framed meridians. Blowing down the two meridians will return the old surgery framing -1 of K; the resulting situation is shown in Figure 6.

For $m = 0$, this is the same picture as in [22, Figure 3]. For $m \geq 1$, blowing down K will increase the surgery framing of the next unknot in the chain to -1. We continue in this fashion with $m-1$ further blow-downs until we reach the same picture as in the case $m = 0$. The further Kirby moves that turn this into the picture of a left-handed trefoil in S^3 are shown in Figures 3 and 4 of [22]. $\qquad\square$
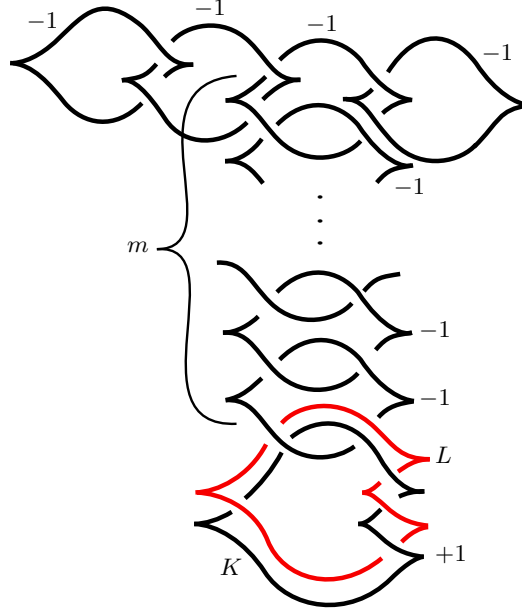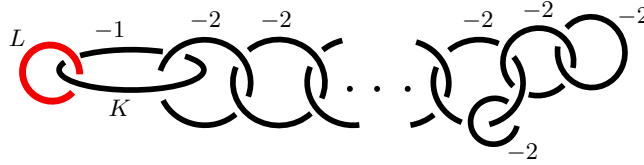
FIGURE 5. Exceptional left-handed trefoils with $\mathtt{tb} = m - 5$.

FIGURE 6. The topological picture for Figures 4 and 5.

Lemma 5.5. *The Legendrian knot L in Figure 5 has $\mathtt{tb}(L) = m-5$ and, depending on a choice of orientation, $\mathtt{rot}(L) = \pm(m - 6)$.*

Proof. Although the final topological picture does not change by adding Legendrian unknots with $\mathtt{tb} = -1$ and contact surgery coefficient -1 to the vertical chain in Figure 5, each of these unknots, when it is blown down, increases the framing of L by one. It therefore suffices to show that $\mathtt{tb}(L) = -5$ for the Legendrian knot L shown in Figure 4, which can be done with the formula from [28, Lemma 6.6], cf. [21, Lemma 3.1] and [11].

Let M be the linking matrix of the surgery diagram in Figure 4. When we order the surgery knots as $L_1, \ldots, L_4$ from left to right and orient them clockwise, this linking matrix is

$$M = \begin{pmatrix} -2 & 1 & 0 & 0 \\ 1 & -2 & 1 & 0 \\ 0 & 1 & -1 & 1 \\ 0 & 0 & 1 & -2 \end{pmatrix}.$$

The extended linking matrix M_0 is defined by including L as the first knot in the diagram, with self-linking number set to zero:

$$M_0 = \begin{pmatrix} 0 & 0 & 1 & -2 & 1 \\ 0 & -2 & 1 & 0 & 0 \\ 1 & 1 & -2 & 1 & 0 \\ -2 & 0 & 1 & -1 & 1 \\ 1 & 0 & 0 & 1 & -2 \end{pmatrix}.$$

Write $\mathtt{tb}_0$ for the Thurston–Bennequin invariant of L as a knot in the unsurgered copy of S^3. Then the formula from [28] for the Thurston–Bennequin invariant of the left-handed trefoil knot L in the surgered copy of S^3 gives

$$(3) \qquad \begin{aligned} \mathtt{tb}(L) &= \mathtt{tb}_0 + \frac{\det M_0}{\det M} \\ &= -2 + \frac{3}{-1} = -5. \end{aligned}$$

For the rotation number $\mathtt{rot}(L)$ of L in the surgered S^3 we also have a formula from [28]; cf. [11]. Write $\mathtt{rot}_0$ for the rotation number of L in the unsurgered copy of S^3. Then

$$(4) \qquad \begin{aligned} \mathtt{rot}(L) &= \mathtt{rot}_0 - \left\langle \begin{pmatrix} \mathtt{rot}(L_1) \\ \vdots \\ \mathtt{rot}(L_4) \end{pmatrix}, M^{-1} \begin{pmatrix} \mathtt{lk}(L, L_1) \\ \vdots \\ \mathtt{lk}(L, L_4) \end{pmatrix} \right\rangle \\ &= 1 - \left\langle \begin{pmatrix} 0 \\ 0 \\ 1 \\ 0 \end{pmatrix}, M^{-1} \begin{pmatrix} 0 \\ 1 \\ -2 \\ 1 \end{pmatrix} \right\rangle \\ &= \langle (0,0,1,0)^{\mathtt{t}}, (-2,-4,-5,-3)^{\mathtt{t}} \rangle = 1 + 5 = 6. \end{aligned}$$

The computation of the rotation number for the general case shown in Figure 5 is analogous, see Section 8.1. $\qquad\square$

Notice that for $m = 6$, when $\mathtt{tb}(L) = 1$, we have $\mathtt{rot}(L) = 0$, so we cannot distinguish the two orientations of L.

The lacuna in the classification of tight contact structures on the trefoil complement prevents us from concluding that the examples for $m \geq 1$ constitute a comprehensive list in the range $\mathtt{tb} > -5$.

The next lemma says that L lives in an overtwisted contact structure, and as the push-off of the single contact $(+1)$-surgery curve, it must then be strongly exceptional by Proposition 2.3. This completes the proof of Theorem 1.5.

Lemma 5.6. *The Legendrian knot L in Figure 5 lives in the overtwisted contact structure $\xi_{3/2}$.*

Proof. We carry out the computation for the case $m = 0$ shown in Figure 4; for the general case see Section 8.1. Read as a Kirby diagram, there are four 2-handles in this figure, so it describes a 2-handlebody X of Euler characteristic $\chi(X) = 5$. The signature of this 4-manifold X is $\sigma(X) = -2$. This can be computed as the signature of the linking matrix M; better, it can be determined by keeping track of the (positive or negative) blow-ups during the Kirby moves. By [9, Corollary 3.6],

the d_3-invariant of the contact structure ξ described by the surgery diagram is then given by

$$(5) \qquad d_3(\xi) = \frac{1}{4}\big(c^2 - 3\sigma(X) - 2\chi(X)\big) + q,$$

where q denotes the number of contact $(+1)$-surgeries (here $q = 1$), and $c \in H^2(X; \mathbb{Z})$ is the cohomology class which evaluates as $\texttt{rot}(L_i)$ on the homology generator of X defined by a Seifert surface of the surgery knot L_i glued with the core disc in the corresponding 2-handle. Write $\underline{\texttt{rot}}$ for the vector of rotation numbers of the L_i. Then the square $c^2 \in \mathbb{Z}$ is found as $c^2 = \mathbf{x}^{\texttt{t}} M \mathbf{x}$, where $\mathbf{x}$ is a solution of the linear equation $M\mathbf{x} = \underline{\texttt{rot}}$.

In our situation, we have $\underline{\texttt{rot}} = (0,0,1,0)^{\texttt{t}}$ and $\mathbf{x} = (2,4,6,3)^{\texttt{t}}$. This gives $c^2 = \mathbf{x}^{\texttt{t}}\underline{\texttt{rot}} = 6$ and

$$d_3(\xi) = \frac{1}{4}(6 + 6 - 10) + 1 = 3/2,$$

that is, $\xi = \xi_{3/2}$. $\qquad\qquad\qquad\qquad\qquad\qquad\qquad\qquad\qquad\qquad\square$

6. Exceptional right-handed trefoils

We now consider Legendrian realisations L of the right-handed trefoil, i.e. the $(2,3)$-torus knot. We show that any value of $\texttt{tb}$ can be realised by an exceptional right-handed trefoil, and we give a complete classification for one value of $\texttt{tb}$.

By Section 4.2.1, for $\texttt{tb}(L) = 7$ the knot complement is the Seifert manifold

$$M\Big(D^2; \frac{1}{2}, \frac{1}{3}\Big) \quad \text{of boundary slope} \quad s = 2.$$

Computing as in Section 5.1.1, where now $-1/r_2 = -3$ gives us $a_0^2 = -3$, one finds that there are at most four strongly exceptional realisations.

Proposition 6.1. *There are exactly four strongly exceptional realisations L of the right-handed trefoil knot with $\texttt{tb}(L) = 7$. They are shown in Figure 7 (with either orientation of L).*
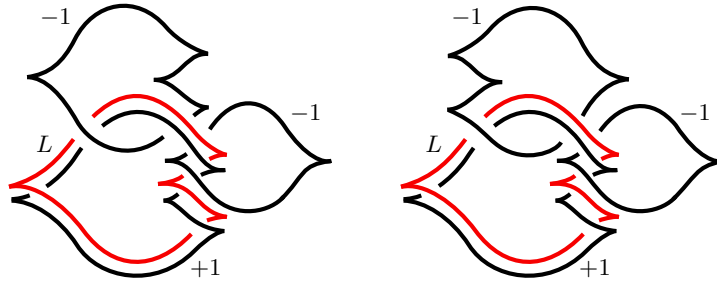

FIGURE 7. The four right-handed exceptional trefoils with $\texttt{tb} = 7$.

Proof. Topologically, the surgery diagram consists of a chain of three unknots with surgery coefficients $-3, -1, -2$. After thrice blowing down a (-1)-curve we obtain the 3-sphere. This also shows that the handlebody X described by the diagram has signature $\sigma(X) = -3$.

The Kirby moves for showing that L is topologically a right-handed trefoil in the surgered S^3 are analogous to those in the proof of Lemma 5.4.

Straightforward computations yield the following classical invariants and d_3-invariant. The Legendrian realisation L on the left in Figure 7 has $(\mathtt{tb}, \mathtt{rot}) = (7, \pm 4)$; the one on the right, $(\mathtt{tb}, \mathtt{rot}) = (7, \pm 8)$. The overtwisted contact structure of the surgered S^3 on the left is $\xi_{1/2}$; on the right, $\xi_{-3/2}$.   □

Although we have no tools yet to classify exceptional right-handed trefoils L with $\mathtt{tb}(L) \neq 7$, we can say something about their existence for all values of $\mathtt{tb}$.

An example with $(\mathtt{tb}, \mathtt{rot}) = (6, \pm 7)$ in $(S^3, \xi_{-3/2})$ has been described in [28, Figure 9]. With one of its orientations, this has non-zero LOSS invariant, so by taking negative stabilisations (and then either orientation) we obtain a pair of exceptional right-handed trefoils for all values of $\mathtt{tb} \leq 6$. By putting the two zigzags of the stabilised knot in [28, Figure 9] to the other side, or one zigzag on either side, one obtains exceptional right-handed trefoils in $(S^3, \xi_{1/2})$ with $(\mathtt{tb}, \mathtt{rot}) = (6, \pm 1)$ and $(6, \pm 3)$, respectively. We do not know, however, whether these new examples have non-zero LOSS invariant.

The first examples with $\mathtt{tb} > 7$ are shown in Figure 8. For $m = 0$ these examples reduce to those in Figure 7, and the same argument as for the left-handed trefoils shows why the value of the Thurston–Bennequin invariant takes the value $m + 7$. The computation of the other invariants is completely standard, and we only give the results in Table 1. We summarise our findings in the following proposition.

Proposition 6.2. *Any integer can be realised as the Thurston–Bennequin invariant of a strongly exceptional Legendrian realisation of the right-handed trefoil. All the known examples for $\mathtt{tb} \leq 5$ live in $\xi_{-3/2}$. For each $\mathtt{tb} \geq 6$, there are examples in $\xi_{-3/2}$ and $\xi_{1/2}$.*   □
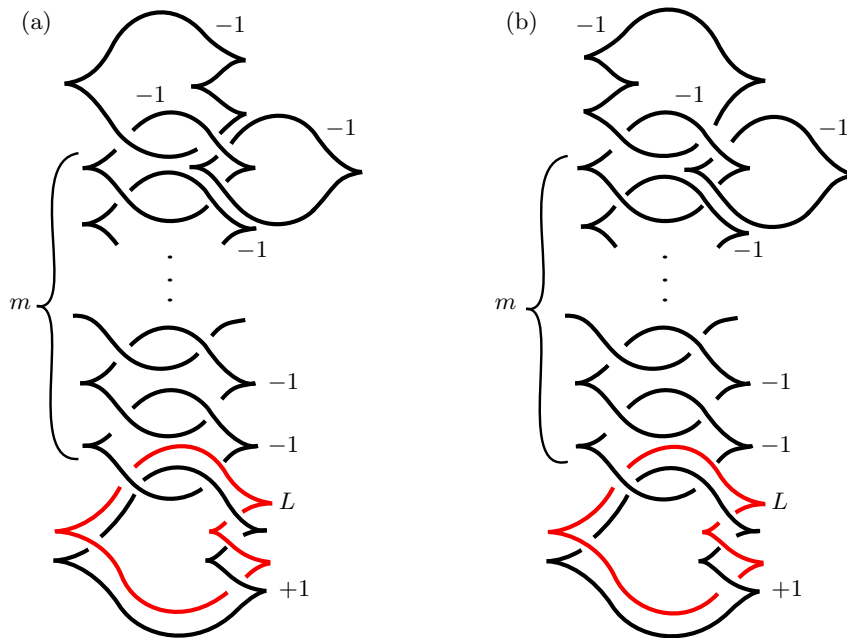

FIGURE 8. Right-handed exceptional trefoils with $\mathtt{tb} > 7$.

Figure	m	tb	rot	d_3
8(a)	odd	$m+7$	$\pm(m+1)$	$-3/2$
8(a)	even	$m+7$	$\pm(m-3)$	$1/2$
8(b)	odd	$m+7$	$\pm(m-3)$	$1/2$
8(b)	even	$m+7$	$\pm(m+1)$	$-3/2$

TABLE 1. Invariants of the right-handed trefoils in Figure 8.

7. GENERAL TORUS KNOTS

In this section we prove two classification results for strongly exceptional realisations of general torus knots.

Proposition 7.1. *For $p \geq 2$ and $n \geq 1$, there are exactly $2p$ strongly exceptional Legendrian realisations L of the $(p, np+1)$-torus knot with $\mathtt{tb}(L) = np^2 + p + 1$. They are shown in Figure 9 (with either orientation of L), where $k, l \in \mathbb{N}_0$ with $k + l = p - 1$. The rotation number of these knots is*

$$\mathtt{rot}(L) = \pm\big(np^2 + p - np(l - k)\big).$$

The ambient overtwisted contact structure ξ is determined by

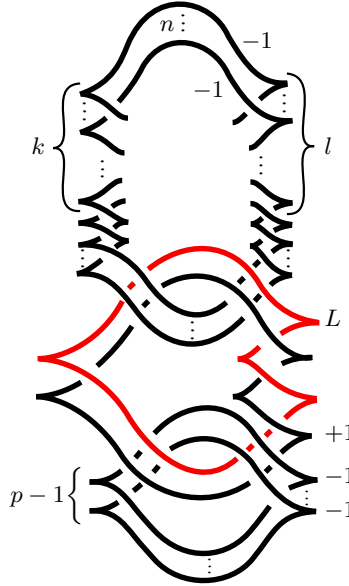$$d_3(\xi) = \frac{n}{4}\big(1 - (p - l + k)^2\big) + \frac{1}{2}.$$

FIGURE 9. The $2p$ exceptional $(p, np+1)$-torus knots with $\mathtt{tb} = np^2 + p + 1$.

Proof. In the notation of Section 4.2.1 we have Seifert invariants $r_1 = (p-1)/p$ and $r_2 = n/(np+1)$, and boundary slope $s = 2$. With the continued fraction expansions

$$-\frac{1}{r_1} = \underbrace{[-2, \ldots, -2]}_{p-1} \quad \text{and} \quad -\frac{1}{r_2} = [-(p+1), \underbrace{-2, \ldots, -2}_{n-1}]$$

the formula in Section 5.1.1 tells us there are $2p$ contact structures of zero Giroux torsion on the knot complement. So we need only verify that Figure 9 does indeed show $2p$ distinct strongly exceptional realisations of the $(p, np + 1)$-torus knot.

Topologically, we transform the diagram by the same procedure as that used at the beginning of Lemma 5.4. This produces a Kirby diagram as in [31, Figure 18], and the further Kirby moves pictured there demonstrate that L is a $(p, np+1)$-torus knot in S^3.

The classical invariants of L and the d_3-invariant of the ambient contact structure are computed in Section 8.2. The $2p$ realisations are distinguished by the rotation number. $\square$

Remark 7.2. We take the opportunity to point out a minor correction to Figure 18 of [31]. The $n-1$ meridians with surgery framing -2 ought to link one another -1 times.

Proposition 7.3. *For $p \geq 2$ and $n \geq 2$, there are exactly $2(p-1)(n-1)$ strongly exceptional realisations L of the $(p, -(np-1))$-torus knot with $\mathtt{tb}(L) = -np^2+p+1$. They are shown in Figure 10 (with either orientation of L), where $k, l, u, v \in \mathbb{N}_0$ with $k+l = p-2$ and $u+v = n-2$. The rotation number of these knots is*

$$\mathtt{rot}(L) = \pm\big(np^2 - p - np(l-k) + p(v-u)\big).$$

The ambient overtwisted contact structure ξ is determined by

$$d_3(\xi) = \frac{1}{4}\big(n(p-l+k)^2 + 2(p-l+k)(v-u)\big) - \frac{1}{2}.$$

Proof. The Seifert invariants are $r_1 = p/(p-1)$ and $r_2 = n/(np-1)$, and the boundary slope is $s = 2$. We have the continued fraction expansions

$$-\frac{1}{r_1} = \underbrace{[-2, \ldots, -2]}_{p-1} \quad \text{and} \quad -\frac{1}{r_2} = [-p, -n].$$

The formula in Section 5.1.1 gives us $2(p-1)(n-1)$ distinct contact structures of zero Giroux torsion on the knot complement. Thus, we need to verify that Figure 10 shows $2(p-1)(n-1)$ distinct Legendrian realisations of the $(p, -(np-1))$-torus knot.

As before, topologically we transform L into a meridian of the parallel knot. We then have the same diagram as in [22, Figure 7], where it is shown that L is a $(p, -(np-1))$-torus knot.

For the remaining calculations see Section 8.3. $\square$

Remark 7.4. (1) By [16, Theorem 4.1], the maximal Thurston–Bennequin invariant for realisations of the (p, q)-torus knot in (S^3, ξ_{st}) is

$$\overline{\mathtt{tb}}_{(p,q)} = pq - p - q \ \text{ for } p, q > 0$$

and

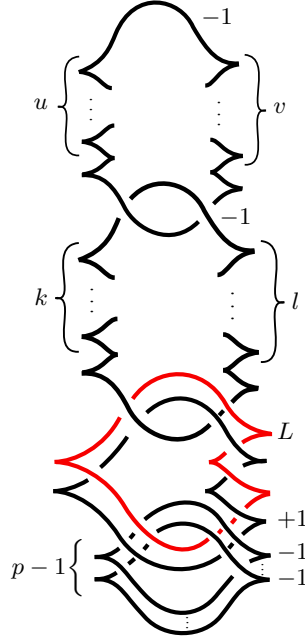$$\overline{\mathtt{tb}}_{(p,q)} = pq \ \text{ for } p > 0, q < 0.$$

FIGURE 10. The $2(n-1)(p-1)$ exceptional $(p, -(np-1))$-torus knots with $\mathtt{tb} = -np^2 + p + 1$.

In particular, we have

$$\overline{\mathtt{tb}}_{(p, np+1)} = np^2 - np - 1 < np^2 + p + 1$$

and

$$\overline{\mathtt{tb}}_{(p, -(np-1))} = -np^2 + p < -np^2 + p + 1,$$

from which we can deduce directly that the contact structures on S^3 described by the surgery diagrams in Figures 9 and 10 must be overtwisted.

(2) Alternative descriptions of the exceptional $(p, -(np-1))$-torus knots can be found in [22, Figure 6]. In that paper, we showed that, ignoring the orientation of L, the $(p-1)(n-1)$ realisations can be distinguished by the result of performing contact (-1)-surgery on them: one obtains the lens space $L(np^2 - p + 1, p^2)$ with $(p-1)(n-1)$ pairwise homotopically distinct contact structures, detected by the Euler class. To distinguish the different orientations of L, one needs the rotation number.

8. Some computations

In this section we collect a few more details about the calculations in the general cases of the previous sections.

8.1. **Left-handed trefoils.** For the computation of the rotation number in Lemma 5.5 for arbitrary m we order the knots in the surgery diagram (Figure 5) from the bottom to the top of the vertical chain, followed by the three knots at the top, starting at the right. Then the linking matrix M (with all knots oriented clockwise) becomes

$$M = \begin{pmatrix} -1 & \overbrace{-1 \quad 0 \quad \ldots \quad 0 \quad \ldots \quad \ldots \quad \ldots}^{m} & 0 \\ -1 & -2 & -1 & \ddots & 0 & \ldots & \ldots & \ldots & \vdots \\ 0 & -1 & -2 & \ddots & 0 & \ldots & \ldots & \ldots & \vdots \\ \vdots & 0 & -1 & \ddots & -1 & 0 & \ldots & \ldots & \vdots \\ \vdots & \vdots & 0 & \ddots & -2 & -1 & 0 & 0 & 0 \\ \vdots & \vdots & \vdots & \ddots & -1 & -2 & 1 & 1 & 0 \\ \vdots & \ldots & \ldots & \ldots & 0 & 1 & -2 & 0 & 0 \\ \vdots & \ldots & \ldots & \ldots & 0 & 1 & 0 & -2 & 1 \\ 0 & \ldots & \ldots & \ldots & 0 & 0 & 0 & 1 & -2 \end{pmatrix}.$$

The vectors of rotation and linking numbers, with L oriented clockwise, too, are

$$\underline{\mathrm{rot}} = (1, 0, \ldots, 0)^{\mathrm{t}} \quad \text{and} \quad \underline{\mathrm{lk}} = (-2, -1, 0, \ldots, 0)^{\mathrm{t}},$$

respectively. By the formula (4) for $\mathrm{rot}(L)$ in the proof of Lemma 5.5 (or rather the obvious generalisation of this formula to any number of surgery knots), we need only compute the first entry of $M^{-1}\underline{\mathrm{lk}}$, for which it suffices to know the first row of M^{-1}. By the symmetry of M (and hence M^{-1}), this is the same as the first column of M^{-1}, that is, $M^{-1}(1, 0, \ldots, 0)^{\mathrm{t}}$.

It is easy to verify that $\mathbf{x} := M^{-1}(1, 0, \ldots, 0)^{\mathrm{t}}$ equals

$$\mathbf{x} = \big(6 - m, -(7 - m), 8 - m, \ldots, (-1)^m \cdot 6, (-1)^m \cdot 3, (-1)^m \cdot 4, (-1)^m \cdot 2\big)^{\mathrm{t}}.$$

Then

$$\mathrm{rot}(L) = 1 - (-2, -1, 0, \ldots, 0)\mathbf{x} = 6 - m.$$

Next we compute the d_3-invariant for the surgered S^3 shown in Figure 5, which we claimed in Lemma 5.6 to equal $3/2$ for all $m \in \mathbb{N}$. For $m = 0$ we had $\chi(X) = 5$ and $\sigma(X) = -2$. Each additional 2-handle adds 1 to the Euler characteristic, so the corresponding handlebody X_m has $\chi(X_m) = m + 5$. The additional surgery curves correspond to negative blow-ups, which gives $\sigma(X_m) = -2 - m$. The square of the first Chern class is computed as $\mathbf{x}^{\mathrm{t}} M \mathbf{x}$, where $\mathbf{x}$ is a solution of $M\mathbf{x} = \underline{\mathrm{rot}}$. So this is indeed the vector $\mathbf{x}$ we have found above, which yields $c^2 = 6 - m$. Putting this information into the formula (5) for d_3 we find the the claimed value.

8.2. **Positive torus knots.** In Figure 9 we take the 'shark' parallel to L as the first knot, followed by the n parallel unknots at the top and the $p-1$ parallel unknots at the bottom. Then the linking matrix M (with all knots oriented clockwise) takes the form

$$M = \begin{pmatrix} -1 & \overbrace{-1 \quad \ldots \quad -1}^{n} & \overbrace{-1 \quad \ldots \quad -1}^{p-1} \\ -1 & -p-1 & \ldots & -p & 0 & \ldots & 0 \\ \vdots & \vdots & \ddots & \vdots & \vdots & \vdots & \vdots \\ -1 & -p & \ldots & -p-1 & 0 & \ldots & 0 \\ -1 & 0 & \ldots & 0 & -2 & \ldots & -1 \\ \vdots & \vdots & \vdots & \vdots & \vdots & \ddots & \vdots \\ -1 & 0 & \ldots & 0 & -1 & \ldots & -2 \end{pmatrix}.$$

Here all off-diagonal elements in the two quadratic subblocks of size n and $p - 1$ are $-p$ and -1, respectively.

By elementary row and column reduction one checks that $\det M = (-1)^{n+p}$. Similarly, for the extended matrix M_0 (as defined in the proof of Lemma 5.5), one finds $\det M_0 = (-1)^{n+p}(np^2 + p + 3)$. With (3) this yields

$$\mathtt{tb}(L) = \mathtt{tb}_0 + \frac{\det M_0}{\det M} = np^2 + p + 1.$$

In order to compute the rotation number with formula (4), we first need to determine $M^{-1}\underline{\mathtt{lk}}$, where $\underline{\mathtt{lk}} = (-2, -1, \ldots, -1)^{\mathtt{t}}$ is the vector of linking numbers of L with the $n + p$ surgery knots. This computation can be simplified by summing over the two boxes of size n and $p - 1$ in M. Thus, we define the 'deflated' matrix

$$M' := \begin{pmatrix} -1 & -n & -p+1 \\ -1 & -np-1 & 0 \\ -1 & 0 & -p \end{pmatrix}$$

and solve the equation $M'\mathbf{y} = (-2, -1, -1)^{\mathtt{t}}$. Notice that $(-2, -1, -1)^{\mathtt{t}}$ is the deflated vector of linking numbers. This gives

$$\mathbf{y} = (np^2 + p + 1, -p, -np - 1)^{\mathtt{t}}.$$

Write $\underline{\mathtt{rot}} = (1, l - k, 0)^{\mathtt{t}}$ for the deflated vector of rotation numbers. With formula (4) we obtain

$$\mathtt{rot}(L) = \mathtt{rot}_0 - \underline{\mathtt{rot}}^{\mathtt{t}} \begin{pmatrix} 1 & 0 & 0 \\ 0 & n & 0 \\ 0 & 0 & p-1 \end{pmatrix} \mathbf{y} = np(l - k) - np^2 - p,$$

or the negative of that for the counter-clockwise orientation of L. As k and l range over $\mathbb{N}_0$ subject to the condition $k + l = p - 1$, some simple arithmetic shows that this gives $2p$ distinct values for the rotation number.

Remark 8.1. The contact (-1)-surgeries along the n or $p - 1$ parallel knots in Figure 9 (which are Legendrian push-offs of one another) are equivalent, by the algorithm of [9], to a contact $(-1/n)$- or $(-1/(p-1))$-surgery along a single copy of the respective knot. For diagrams involving contact $(1/k)$-surgeries, $k \in \mathbb{Z}$, one can directly apply the formula in [11, Theorem 2.2] to compute $\mathtt{rot}(L)$. For the diagram at hand, that formula is identical to the one we obtained above by 'deflation'.

For the computation of the d_3-invariant we first observe that the handlebody X described by the surgery diagram in Figure 9 has Euler characteristic $\chi(X) = 1 + n + p$, since the number of 2-handles is $n + p$, and signature $\sigma(X) = -n - p$, as can be seen from the $n + p$ negative blow-downs during the Kirby moves in [31, Figure 18]. The solution $\mathbf{x}$ of the equation $M'\mathbf{x} = \underline{\mathtt{rot}}$ is

$$\mathbf{x} = \begin{pmatrix} -np^2 + np(l - k) - p \\ p - (l - k) \\ np - n(l - k) + 1 \end{pmatrix}.$$

This gives

$$c^2 = \mathbf{x}^{\mathtt{t}} \begin{pmatrix} 1 & 0 & 0 \\ 0 & n & 0 \\ 0 & 0 & p-1 \end{pmatrix} \underline{\mathtt{rot}} = -n(p - l + k)^2 - p.$$

The formula (5) for the d_3-invariant (in the proof of Lemma 5.6) then yields the value of d_3 as claimed in Proposition 7.1. Notice that the d_3-invariant never attains the value $-1/2 = d_3(\xi_{st})$, so the contact structures on S^3 given by these surgery diagrams are overtwisted.

Remark 8.2. (1) We may check our calculation of the d_3-invariant against the formula in [11, Theorem 5.1] by translating the surgeries in Figure 9 into rational surgeries as explained in Remark 8.1. Our deflated matrix M' is precisely the matrix Q on page 525 of [11], obtained from the rational surgery coefficients. The characteristic polynomial of this matrix has three negative real roots, so in the notation of [11] we have $\sigma(M') = -3$. The rational contact surgery coefficients are $+1$, $-1/n$, and $-1/(p-1)$. Plugging this into the formula of [11, Theorem 5.1], we obtain

$$
\begin{aligned}
d_3(\xi) &= \frac{1}{4}\big(c^2 + (3-1) - (3-n) - (3-(p-1))\big) - \frac{3}{4}\sigma(M') - \frac{1}{2} \\
&= \frac{n}{4}\big(1 - (p-l+k)^2\big) + \frac{1}{2},
\end{aligned}
$$

as in Proposition 7.1.

(2) A formula for computing the Thurston–Bennequin invariant of Legendrian knots represented in surgery diagrams involving rational contact surgeries was found in [27]. This formula tells us that, with $\underline{\mathtt{lk}} = (-2,-1,-1)^{\mathtt{t}}$ denoting the vector of linking numbers in the rational diagram (i.e. the deflated vector),

$$
\mathtt{tb}(L) = \mathtt{tb}_0 - \mathbf{y}^{\mathtt{t}} \begin{pmatrix} 1 & 0 & 0 \\ 0 & n & 0 \\ 0 & 0 & p-1 \end{pmatrix} \underline{\mathtt{lk}} = np^2 + p + 1,
$$

confirming our earlier computation.

8.3. **Negative torus knots.** In Figure 10 we take the knot parallel to L as the first knot, followed by the $p-1$ unknots at the bottom, and finally the two knots above L. With all knots oriented clockwise, the linking matrix is

$$
M = \begin{pmatrix}
-1 & \overbrace{-1}^{p-1} & \dots & -1 & -1 & 0 \\
-1 & -2 & \dots & -1 & 0 & 0 \\
\vdots & \vdots & \ddots & \vdots & \vdots & \vdots \\
-1 & -1 & \dots & -2 & 0 & 0 \\
-1 & 0 & \dots & 0 & -p & -1 \\
0 & 0 & \dots & 0 & -1 & -n
\end{pmatrix}.
$$

This has $\det M = (-1)^{p+1}$, and the determinant of the extended matrix M_0 is $\det M_0 = (-1)^{p-1}(-np^2 + p + 3)$. By (3) the Thurston–Bennequin invariant of L in the surgered S^3 is

$$
\mathtt{tb}(L) = \mathtt{tb}_0 + \frac{\det M_0}{\det M} = -np^2 + p + 1.
$$

We now sum over the quadratic subblock of size $p-1$ to obtain the deflated matrix

$$
M' := \begin{pmatrix}
-1 & -p+1 & -1 & 0 \\
-1 & -p & 0 & 0 \\
-1 & 0 & -p & -1 \\
0 & 0 & -1 & -n
\end{pmatrix}.
$$

The deflated vectors of rotation numbers and linking numbers are

$$\underline{\tt rot} = (1, 0, l - k, v - u)^{\tt t} \quad \text{and} \quad \underline{\tt lk} = (-2, -1, -1, 0)^{\tt t},$$

respectively. The solution $\mathbf{y}$ of $M'\mathbf{y} = \underline{\tt lk}$ is

$$\mathbf{y} = \begin{pmatrix} -np^2 + p + 1 \\ np - 1 \\ np \\ -p \end{pmatrix},$$

so we find

$$\mathtt{rot}(L) = \mathtt{rot}_0 - \underline{\tt rot}^{\tt t} \begin{pmatrix} 1 & 0 & 0 & 0 \\ 0 & p - 1 & 0 & 0 \\ 0 & 0 & 1 & 0 \\ 0 & 0 & 0 & 1 \end{pmatrix} \mathbf{y} = np^2 - p - np(l - k) + p(v - u),$$

or the negative of that for the counter-clockwise orientation of L. For the different choices of (k, l) and (u, v), these $2(p - 1)(n - 1)$ rotation numbers are pairwise distinct and distinguish the Legendrian realisations.

The number of 2-handles is $p + 2$, so the handlebody X described by the Kirby diagram in Figure 10 has $\chi(X) = p + 3$. From the Kirby moves in [22, Figure 7] one reads off that $\sigma(X) = 1 - (p + 1) = -p$. The solution of the equation $M'\mathbf{x} = \underline{\tt rot}$ is

$$\mathbf{x} = \begin{pmatrix} np^2 - p - np(l - k) + p(v - u) \\ -np + 1 + n(l - k) - (v - u) \\ -np + n(l - k) - (v - u) \\ p - (l - k) \end{pmatrix}.$$

We then compute

$$c^2 = \mathbf{x}^{\tt t} \begin{pmatrix} 1 & 0 & 0 & 0 \\ 0 & p - 1 & 0 & 0 \\ 0 & 0 & 1 & 0 \\ 0 & 0 & 0 & 1 \end{pmatrix} \underline{\tt rot} = n(p - l + k)^2 + 2(p - l + k)(v - u) - p.$$

Putting all this information into the formula (5) for d_3 gives the value claimed in Proposition 7.3. Again we observe that the d_3-invariant never takes the value $-1/2$.

REFERENCES

[1] K. BAKER AND J. ETNYRE, Rational linking and contact geometry, *Perspectives in Analysis, Geometry, and Topology*, Progr. Math. **296** (Birkhäuser Verlag, Basel, 2012), 19–37.

[2] K. L. BAKER AND S. ONARAN, Nonlooseness of nonloose knots, *Algebr. Geom. Topol.* **15** (2015), 1031–1066.

[3] YU. CHEKANOV, Differential graded algebra of Legendrian links, *Invent. Math.* **150** (2002), 441–483.

[4] F. CHEN, F. DING AND Y. LI, Legendrian torus knots in $S^1 \times S^2$, *J. Knot Theory Ramifications* **24** (2015), 1550064, 14pp.

[5] F. Ding and H. Geiges, A Legendrian surgery presentation theorem of contact 3-manifolds, *Math. Proc. Cambridge Philos. Soc.* **136** (2004), 583–598.

[6] F. Ding and H. Geiges, Legendrian knots and links classified by classical invariants, *Commun. Contemp. Math.* **9** (2007), 135–162.

[7] F. Ding and H. Geiges, Handle moves in contact surgery diagrams, *J. Topol.* **2** (2009), 105–122.

[8] F. Ding and H. Geiges, Legendrian helix and cable links, *Commun. Contemp. Math.* **12** (2010), 487–500.

[9] F. Ding, H. Geiges and A. I. Stipsicz, Surgery diagrams for contact 3-manifolds, *Turkish J. Math.* **28** (2004), 41–74.

[10] F. Ding, Y. Li and Q. Zhang, Tight contact structures on some bounded Seifert manifolds with minimal convex boundary, *Acta Math. Hungar.* **139** (2013), 64–84.

[11] S. Durst and M. Kegel, Computing rotation and self-linking number in contact surgery diagrams, *Acta Math. Hungar.* **150** (2016), 524–540.

[12] K. Dymara, Legendrian knots in overtwisted contact structures on S^3, *Ann. Global Anal. Geom.* **19** (2001), 293–305.

[13] Ya. Eliashberg and M. Fraser, Classification of topologically trivial Legendrian knots, *Geometry, Topology, and Dynamics (Montréal, 1995)* CRM Proc. Lecture Notes **15** (American Mathematical Society, Providence, RI, 1998), 17–51.

[14] Ya. Eliashberg and M. Fraser, Topologically trivial Legendrian knots, *J. Symplectic Geom.* **7** (2009), 77–127.

[15] J. B. Etnyre, On knots in overtwisted contact structures, *Quantum Topol.* **4** (2013), 229–264.

[16] J. B. Etnyre and K. Honda, Knots and contact geometry I. Torus knots and the figure eight knot, *J. Symplectic Geom.* **1** (2001), 63–120.

[17] J. B. Etnyre and D. S. Vela-Vick, Torsion and open book decompositions, *Int. Math. Res. Not. IMRN* **2010** (2010), 4385–4398.

[18] D. T. Gay, Four-dimensional symplectic cobordisms containing three-handles, *Geom. Topol.* **10** (2006), 1749–1759.

[19] H. Geiges, *An Introduction to Contact Topology*, Cambridge Stud. Adv. Math. **109** (Cambridge University Press, Cambridge, 2008).

[20] H. Geiges and C. Lange, Seifert fibrations of lens spaces, *Abh. Math. Semin. Univ. Hambg.*, to appear.

[21] H. Geiges and S. Onaran, Legendrian rational unknots in lens spaces, *J. Symplectic Geom.* **13** (2015), 17–50.

[22] H. Geiges and S. Onaran, Legendrian lens space surgeries, *Michigan Math. J.*, to appear.

[23] H. Geiges and K. Zehmisch, How to recognize a 4-ball when you see one, *Münster J. Math.* **6** (2013), 525–554.

[24] P. Ghiggini, Linear Legendrian curves in T^3, *Math. Proc. Cambridge Philos. Soc.* **140** (2006), 451–473.

[25] P. Ghiggini, P. Lisca and A. I. Stipsicz, Tight contact structures on some small Seifert fibered 3-manifolds, *Amer. J. Math.* **129** (2007), 1403–1447.

[26] E. Giroux, Une structure de contact, même tendue, est plus ou moins tordue, *Ann. Sci. École Norm. Sup. (4)* **27** (1994), 697–705.

[27] M. Kegel, The Legendrian knot complement problem, `arXiv:1604.05196`.

[28] P. Lisca, P. Ozsváth, A. I. Stipsicz and Z. Szabó, Heegaard Floer invariants of Legendrian knots in contact three-manifolds, *J. Eur. Math. Soc. (JEMS)* **11** (2009), 1307–1363.

[29] P. Lisca and A. I. Stipsicz, Ozsváth–Szabó invariants and tight contact three-manifolds I, *Geom. Topol.* **8** (2004), 925–945.

[30] L. Moser, Elementary surgery along a torus knot, *Pacific J. Math.* **38** (1971), 737–745.

[31] S. Onaran, Invariants of Legendrian knots from open book decompositions, *Int. Math. Res. Not. IMRN* **2010** (2010), 1831–1859.

[32] S. Onaran, Legendrian torus knots in lens spaces, `arXiv:1012.3047`.

[33] A. I. Stipsicz and V. Vértesi, On invariants of Legendrian knots, *Pacific J. Math.* **239** (2009), 157–177.

Mathematisches Institut, Universität zu Köln, Weyertal 86–90, 50931 Köln, Germany
  E-mail address: `geiges@math.uni-koeln.de`

Department of Mathematics, Hacettepe University, 06800 Beytepe-Ankara, Turkey
  E-mail address: `sonaran@hacettepe.edu.tr`